Title
Climate Change Trends and Impacts on Vegetation Greening Over the Tibetan Plateau

Journal
Journal of Geophysical Research: Atmospheres, 124(14)

ISSN
2169-897X

Authors
Zhong, Lei
Ma, Yaoming
Xue, Yongkang
et al.

Publication Date
2019-07-27

DOI
10.1029/2019jd030481

Peer reviewed

JGR Atmospheres

RESEARCH ARTICLE
10.1029/2019JD030481

Climate Change Trends and Impacts on Vegetation Greening Over the Tibetan Plateau

Lei Zhong[1,2,3], **Yaoming Ma**[4,5,6], **Yongkang Xue**[7], **and Shilong Piao**[4,5,8]

[1]School of Earth and Space Sciences, University of Science and Technology of China, Hefei, China, [2]CAS Center for Excellence in Comparative Planetology, Hefei, China, [3]Jiangsu Collaborative Innovation Center for Climate Change, Nanjing, China, [4]Key Laboratory of Tibetan Environment Changes and Land Surface Processes, Institute of Tibetan Plateau Research, The Chinese Academy of Sciences, Beijing, China, [5]CAS Center for Excellence in Tibetan Plateau Earth Sciences, Beijing, China, [6]College of Earth and Planetary Sciences, University of Chinese Academy of Sciences, Beijing, China, [7]Department of Geography, University of California, Los Angeles, CA, USA, [8]Sino-French Institute for Earth System Science, College of Urban and Environmental Sciences, Peking University, Beijing, China

Abstract The Tibetan Plateau (TP) is an ecologically fragile region that is sensitive to climate change. In the context of global climate change, the climate change trends of the TP and the vegetation dynamic response need to be investigated. Based on in situ meteorological data, Satellite Pour l'Observation de la Terre vegetation data, and Moderate Resolution Imaging Spectroradiometer land cover data, a comprehensive analysis was conducted to determine the trends of climate parameters in the TP region at different time scales (long term: 1960–2014; midterm: 1980–2014; short term 1999–2014). A consistent warming trend was observed for different temporal scales, while a warming slowdown was identified during 1999 and 2014. The warming rate was also shown to be much higher in the high-altitude regions (>4,000 m), especially at midterm and short-term time scales. A new cloud-free time series of vegetation index data sets was reconstructed, and the vegetation density showed a general increasing trend along with a warming trend in the TP. The regions showing significant increases accounted for 7.63% of the total Tibetan territory. The major significant greening trend of the TP was mainly caused by climate factors. The reforestation projects may have played a minor role in the vegetation greening in specific regions of the TP. In addition, various vegetation types showed markedly different responses to climate changes. The grassland in semiarid regions, which accounted for 41.9% of the territory of the TP, was identified to be very sensitive to variations in both temperature and precipitation.

Key Points:
- The warming trend was observed at different temporal scales in the TP, while a warming slowdown was identified during 1999 and 2014
- A new cloud-free time series of vegetation index data sets was reconstructed, and the vegetation density showed a general increasing trend
- The grassland in semiarid regions was found to be very sensitive to changes in both temperature and precipitation

Correspondence to:
L. Zhong and Y. Ma,
ymma@itpcas.ac.cn;
zhonglei@ustc.edu.cn

Citation:
Zhong, L., Ma, Y., Xue, Y., & Piao, S. (2019). Climate change trends and impacts on vegetation greening over the Tibetan Plateau. *Journal of Geophysical Research: Atmospheres*, *124*, 7540–7552. https://doi.org/10.1029/2019JD030481

Received 15 FEB 2019
Accepted 19 JUN 2019
Accepted article online 3 JUL 2019
Published online 22 JUL 2019

1. Introduction

The global climate has undergone rapid changes in recent several decades. The Intergovernmental Panel on Climate Change Fifth Assessment Report noted that the global surface air temperature increased by 0.85 °C [0.65–1.06 °C] between 1880 and 2015, while the warming rate from 1951 to 2015 was 0.12 °C [0.10–0.14 °C] per decade, which was twice the warming rate from 1880 to 2015 (Intergovernmental Panel on Climate Change, 2013). Since the end of the 1990s, a so-called "warming hiatus" phenomenon was observed at different locations around the world (Kerr, 2009; Knight et al., 2009; Trenberth & Fasullo, 2013). The phenomenon itself and its underlying mechanisms have been widely discussed by the scientific community (Easterling & Wehner, 2009; Meehl et al., 2011; Kosaka & Xie, 2013; Xie, 2016). Called the "Roof of the World" and "the Third Pole," the Tibetan Plateau (TP) has also experienced intensive climatic changes, which in turn drive complex changes in the hydrological cycle. A series of studies on climate change have been conducted over the TP (An et al., 2012; Kang et al., 2010; Yao et al., 2000). Xu et al. (2008) reported a warming trend over the TP from 1961 to 2001 based on the meteorological data of 38 sites, and their results also showed an increasing precipitation trend. However, the climate change trends over the TP at different time scales, especially in recent years, have not been examined systematically. Some questions remain to be resolved. (1) Has a warming hiatus occurred over the TP? (2) What are the air temperature trends at different altitudes in this region?

Vegetation is a natural "link" between the pedosphere, atmosphere, and hydrosphere, and it can also act as an indicator in global climate change studies. Therefore, dynamic monitoring of vegetation cover can reflect trends in climate change to some extent. The relationship between climate and vegetation is a fundamental and key issue for global climate change and terrestrial ecosystem studies. Relevant research on the above

issues not only provides various parameters for meteorological model establishment but also aids to gain a better understanding of the mechanisms underlying the effects of climate change (i.e., temperature and precipitation) on vegetation. Monitoring vegetation dynamics by remote sensing and analyzing their relationships with climate change has become an important research field for global change studies (Rees et al., 2001). Satellite images have been widely used in monitoring and simulating vegetation coverage dynamics (Liu et al., 2016; Tian et al., 2017). Satellite data are also used to analyze the annual and interannual vegetation changes and verify the simulation results of global dynamic vegetation models. For example, Immerzeel et al. (2005) applied the fast Fourier transform method to process Satellite Pour l'Observation de la Terre (SPOT) Normalized Difference Vegetation Index (NDVI) data to identify the relationships between vegetation variations and precipitation over the TP. Sun et al. (2015) analyzed the vegetation variation trends in North China and revealed the natural and anthropogenic influence based on SPOT NDVI data. The results showed that the vegetation variations in North China were mainly influenced by human activities. Zhu, Zhang, et al. (2016) conducted a field experiment in a Tibetan alpine meadow and found warming caused a seasonal shift of ecosystem C exchange. Huang et al. (2016) verified that the vegetation dynamics in the TP were influenced by climate and human activities. Areas dominated by human activities are much smaller than those dominated by climate. Using daily measurements from a rain gauge, Zhang et al. (2017) found a significant increase in the amount of precipitation over the southeastern TP in May from 1979–2014, which demonstrated the wetting and greening of the TP in early summer in recent decades. Zhu et al. (2016) identified the global greening trends by using ecosystem models and satellite data. Although studies have focused on the vegetation dynamics over the TP based on various remote sensing data (Ding et al., 2007; Wang et al., 2015), most of them have used NDVI data processed by the Maximum Value Composition (MVC) method. The limitation is that cloud effects remain in MVC data, which introduced uncertainties in previous analyses. Moreover, the cloud-free NDVI data reconstructed by Harmonic ANalysis of Time Series (HANTS) algorithm used in this study has a finer spatial resolution of 1 km and the latest temporal coverage up to 2014; thus, these data can provide more details on vegetation dynamics, especially in recent years. Lastly, previous studies did not focus on the vegetation dynamics of different land cover types. In this study, both land cover data and NDVI data have the same spatial resolution of 1 km, which promotes a greater understanding of the vegetation responses to temperature and precipitation over different land surface types.

In summary, the TP climate change trends over different time scales and the vegetation responses are worthy of further investigation by using the latest cloud-free satellite data and in situ meteorological data. This study analyses the TP climate change using a statistical approach based on observational data at different temporal scales (long term from 1960–2014, midterm from 1980–2014, and short term from 1999–2014). In addition, the study of vegetation responses to climate variations in the unique region of the TP were strengthened, and greater attention was paid to the differential responses of various vegetation types.

2. Data and Methods

In situ meteorological data were derived from the Chinese surface monthly climate data set (V3.0) from the Chinese Meteorological Data Network (http://data.cma.gov.cn/). The selected meteorological parameters included air temperature, wind speed, and precipitation. A quality control procedure was conducted to obtain 69 stations for the analysis. Among these 69 stations, 52 stations were located below 4,000 m, while the other 17 stations were located above 4,000 m. The stations for those two groups are listed in Table 1. The other data set was the SPOT vegetation index (Maisongrande et al., 2004), which had a spatial resolution of 1 km (1999–2014). Based on the original 10-day MVC synthetic product, a new time series of a cloud-free data set was constructed by applying the HANTS algorithm. In the HANTS algorithm, cloud removal is combined with a smoothing process using a Fourier analysis, and those pixels identified as cloudy are replaced by a filtered value (Zou et al., 2018). Details on the HANTS algorithm can be found in Verhoef (1996). To quantitatively understand the responses of different underlying surface types (vegetation) to the short-term climate change over the TP, the MCD12Q1 underlying surface classification data (Friedl et al., 2010) were introduced. The vegetation of the underlying surface of the TP was divided into 11 types.

First, time series of the near-surface meteorological dataset were constructed at different temporal scales. A linear fitting method was utilized to simulate the general trend of the constructed time series data. The least squares method was used to calculate the slope and intercept of the fitting equation.

Table 1
Stations Below and Above 4,000 m (Units: Meters)

Station (elevation)	Station (elevation)	Station (elevation)	Station (elevation)	Station (elevation)
Dujiangyan (698.5)	Wudu (1,079.1)	Gaotai (1,332.2)	Jiuquan (1,477.2)	Zhangye (1,482.7)
Wuwei (1,531.5)	Shandan (1,764.6)	Minhe (1,813.9)	Lintao (1,893.8)	Linxia (1,917.2)
Yongchang (1,976.9)	Guizhou (2,237.1)	Xining (2,295.2)	Minxian (2,315.0)	Xiaojin (2,369.2)
Batang (2,589.2)	Kangding (2,615.7)	Maerkang (2,664.4)	Bome (2,736.0)	Xiaozaohuo (2,767.0)
Lenghu (2,770.0)	Qilian (2,787.4)	Nuomuhong (2,790.4)	Germu (2,807.6)	Qiabuqia (2,835.0)
Songpan (2,850.7)	Hezuo (2,910.0)	Mangya (2,944.8)	Delingha (2,981.5)	Xinlong (3,486.0)
Linzhi (2,991.8)	Wushaoling (3,045.1)	Dachaidan (3,173.2)	Dulan (3,191.1)	Gangcha (3,208.0)
Changdu (3,306.0)	Xinghai (3,323.2)	Tuole (3,367.0)	Menyuan (3,486.0)	Zedang (3,551.7)
Jiuzhi (3,628.5)	Nangqian (3,643.7)	Lasha (3,648.9)	Yushu (3,681.2)	Ruoergai (3,439.6)
Rikaze (3,836.0)	Longzi (3,860.0)	Dingqing (3,873.1)	Henan (3,955.0)	Dari (3,967.5)
Suoxian (4,022.8)	*Jiangzi (4,040.0)*	*Zaduo (4,066.4)*	*Qumalai (4,175.0)*	*Maduo (4,272.3)*
Shiquanhe (4,278.6)	*Pali (4,300.0)*	*Daocheng (4,397.0)*	*Qingshuihe (4,415.1)*	*Yeniugou (4,431.0)*
Nagqu (4,507.0)	*Tuotuohe (4,533.1)*	*Wudaoliang (4,612.2)*	*Shenzha (4,672.0)*	*Bange (4,700.0)*
Dege (4,745.0)	*Ganzi (4,843.0)*	*Jiali (4,488.8)*	*Seda (4,149.0)*	

Note. Stations in italics denote elevation above 4,000 m.

$$a = \frac{\sum_{i=1}^{n} y_i t_i - \frac{1}{n}\left(\sum_{i=1}^{n} y_i\right)\left(\sum_{i=1}^{n} t_i\right)}{\sum_{i=1}^{n} t^2 - \frac{1}{n}\left(\sum_{i=1}^{n} t_i\right)^2}, b = \bar{y} - a\bar{t} \tag{1}$$

where $\bar{y} = \frac{1}{n}\sum_{i=1}^{n} y_i, \bar{t} = \frac{1}{n}\sum_{i=1}^{n} t_i$

The Mann-Kendall (M-K) test was then applied to the time series data (Kendall, 1975; Mann, 1945). The M-K method is one of the most widely used nonparametric tests for trend and mutation analyses of time series data. The nature of the M-K test is rank correlation, and the emphasis is on the order rather than the numerical sequence itself. The goal is to compare the number of different sizes of the two series in their respective sequences. In the utility model, the sample does not need to follow a certain distribution and is unaffected by a few outliers.

The sequential version of the M-K test was suggested to detect abrupt changes in the climate variables based on the procedures described by Gerstengarbe and Werner (1999). The test is composed of two series: a progressive statistic variable UF_k and a backward variable UB_k. If the UF_k and UB_k curves cross each other and the intersection of the two series is located beyond the specific threshold value of ± 1.96 or ± 2.58 (significance level of 0.05 or 0.01, respectively), an abrupt change at that point can be inferred.

For monitoring land surface properties, such as vegetation, albedo, and land surface temperature, cloud cover effects should be removed first. Furthermore, artifacts caused by atmospheric haze and residual cloud cover remain visible in the time series of MVC-processed data. Here, the HANTS algorithm was used to reconstruct gapless NDVI time series data (Verhoef, 1996; Wen et al., 2004). HANTS is a comprehensive method of smoothing and filtering, and it can fully exploit the temporal and spatial characteristics of remote sensing images. Fourier decomposition was applied to the reconstructed NDVI time series data to generate amplitude and phase values:

$$y_i = a_0 + \sum_{j=1}^{n/2} a_j \cos\left(\omega_j t + \varphi_j\right) \tag{2}$$

$$\omega_j = \frac{2\pi}{n} \times j \tag{3}$$

where n is the sampling number; i is the ith sampling point of the image; a_j is the Fourier amplitude component; and φ_j is the Fourier phase component.

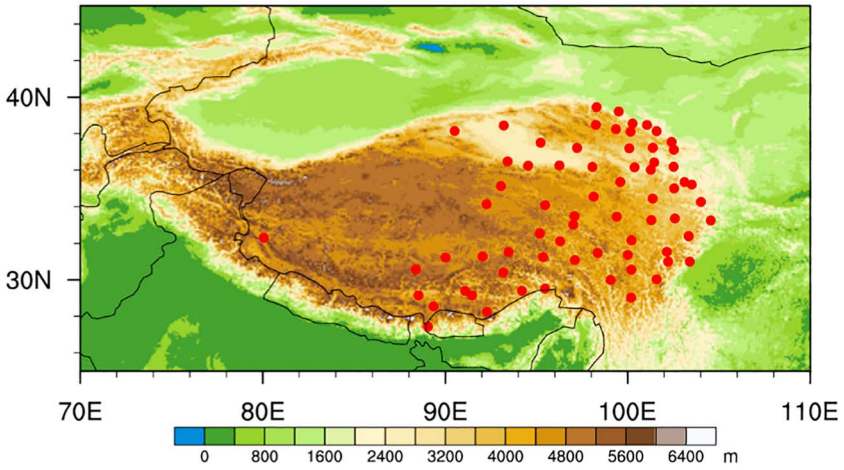

Figure 1. Spatial distributions of meteorological stations over the Tibetan Plateau.

To identify the interannual NDVI changes, a linear trend analysis was performed to identify the plateau NDVI variations.

$$R_{xt} = \frac{\sum_{i=1}^{n}(x_i - \bar{x})(i - \bar{t})}{\sqrt{\sum_{i=1}^{n}(x_i - \bar{x})^2 \sum_{i=1}^{n}(i - t)^2}} \tag{4}$$

where x_i is the NDVI value in the ith year; $\bar{x} = \frac{1}{n}\sum_{i=1}^{n} x_i$, $i = 1, 2, 3, \ldots, n$; and $\bar{t} = \frac{1}{n}\sum_{i=1}^{n} i$. The n is the total number of years. The positive (negative) values of R_{xt} represent the increasing (decreasing) trends of NDVI.

3. Results and Discussion

3.1. Climate Change Trends in the TP

Ground meteorological data were collected from 69 stations in the study area, most of them in the eastern TP (Figure 1). Because of the harsh natural geographical environment in the western TP, few stations have been constructed in this area; however, the Purang and Gaize stations are located in the western TP, and measurements starting from 1979 are available. To avoid uncertainty in the statistical results due to missing data, only the stations with no more than two successive missing monthly records from 1960–2014 were selected. Although point measurements have some limitations in their representativeness, they are superior to other data sets in continuity and precision. The selected stations also cover major climate zones and land cover types in the TP to ensure that our results have good representativeness. The anomalies in the annual mean air temperature, wind speed, and precipitation are shown in Figures 2a, 2c, and 2e, respectively. The annual mean air temperature anomalies showed an overall rising trend over the TP (Figure 2a and Table 2). As shown in the linear fitting curve of the three time periods, the increasing rate between 1980 and 2014 was generally much larger than that of the other two periods. The annual mean in 2014 were 1.27 °C higher than the corresponding 1960–1990 averages. The annual mean air temperature increasing rate between 1960 and 2014 over the TP was approximately 0.03 °C/year, which was slightly higher than that over all of Asia (0.028 °C/year from 1960–2014; Climate Change Center of China Meteorological Administration, 2015) and China (0.0244 ± 0.0021 ° C/year from 1951–2015, Li et al., 2017) for the same period. It is worth noting that since the late 1990s, a so-called "warming hiatus" phenomenon has been observed in different locations around the world. However, in the TP region, warming is still occurring. The evidence indicates that the air temperature over the TP has been increasing by 0.023 °C/year since 1999. However, compared with the warming rate of 0.035 °C/year during 1980 and 1998. A warming slowdown phenomenon can be identified. The trend of increasing temperature on the plateau may be a result of the superposition of many factors. First, because of increases in vegetation density, land surface albedo tends to decrease, which promotes more absorption of solar radiation energy and subsequent warming (Zhong et al., 2011). Meanwhile, the weakening of wind

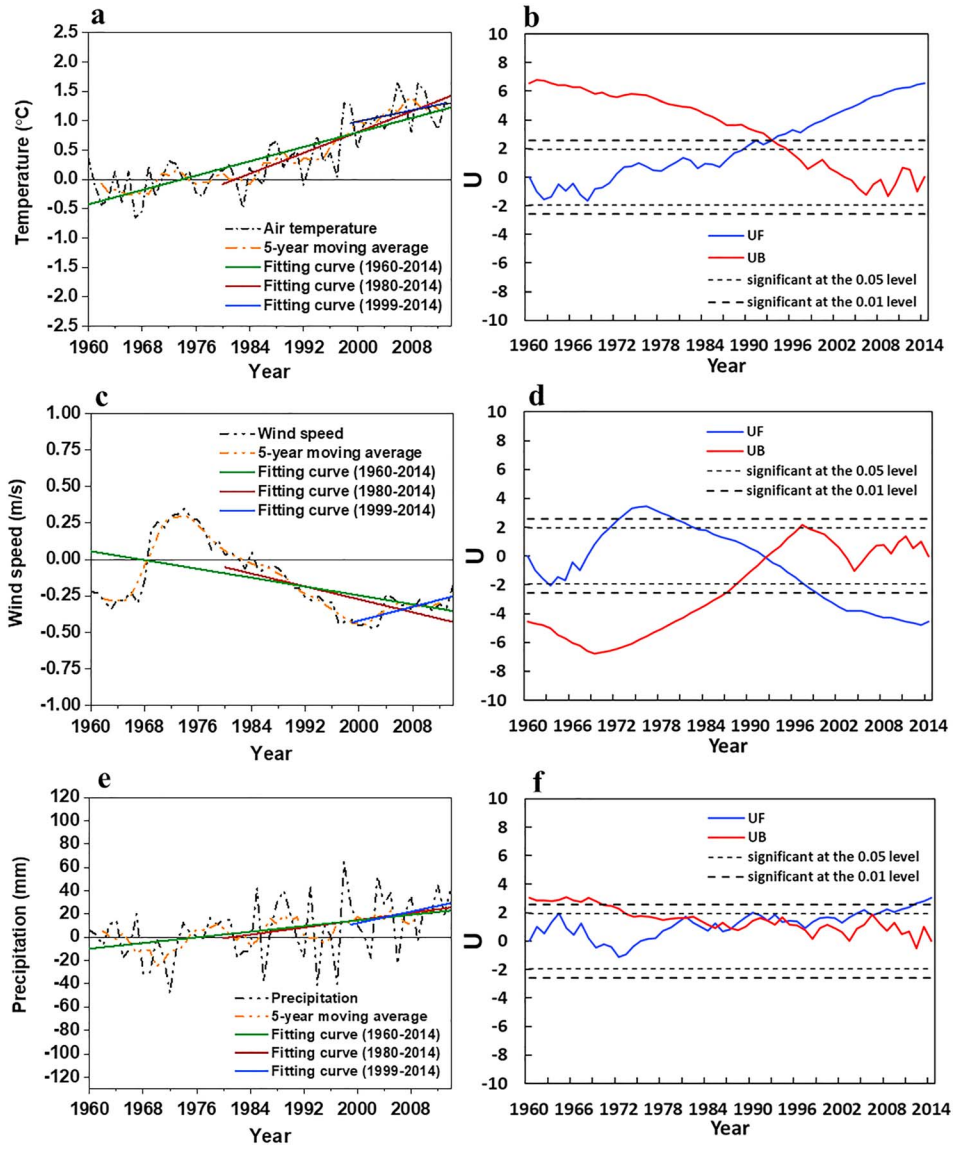

Figure 2. Variations in the annual air temperature anomalies and Mann-Kendall test curves. (a, c, and e) Anomalies in average air temperature, wind speed, and precipitation, respectively; (b, d, and f) Mann-Kendall test curves. "UF" and "UB" are defined in section 2.

Table 2
Air Temperature, Wind Speed, and Precipitation Tendencies at Different Time Scales and Elevations

	1960–2014			1980–2014			1999–2014		
Parameters	Tendency	R^2	Sig	Tendency	R^2	Sig	Tendency	R^2	Sig
Mean air temperature	0.03	0.67	S	0.04	0.67	S	0.02	0.12	I
Mean air temperature (below 4,000 m)	0.03	0.70	S	0.04	0.66	S	0.02	0.08	I
Mean air temperature (above 4,000 m)	0.03	0.58	S	0.05	0.59	S	0.04	0.21	I
Mean wind speed	–0.01	0.27	S	–0.01	0.52	S	0.01	0.45	S
Precipitation	0.61	0.15	S	0.78	0.08	I	1.23	0.07	I

Note. R^2 is a measure of the overall accuracy of the linear regression model in Figure 1.S and I, denoting significance and insignificance, respectively.

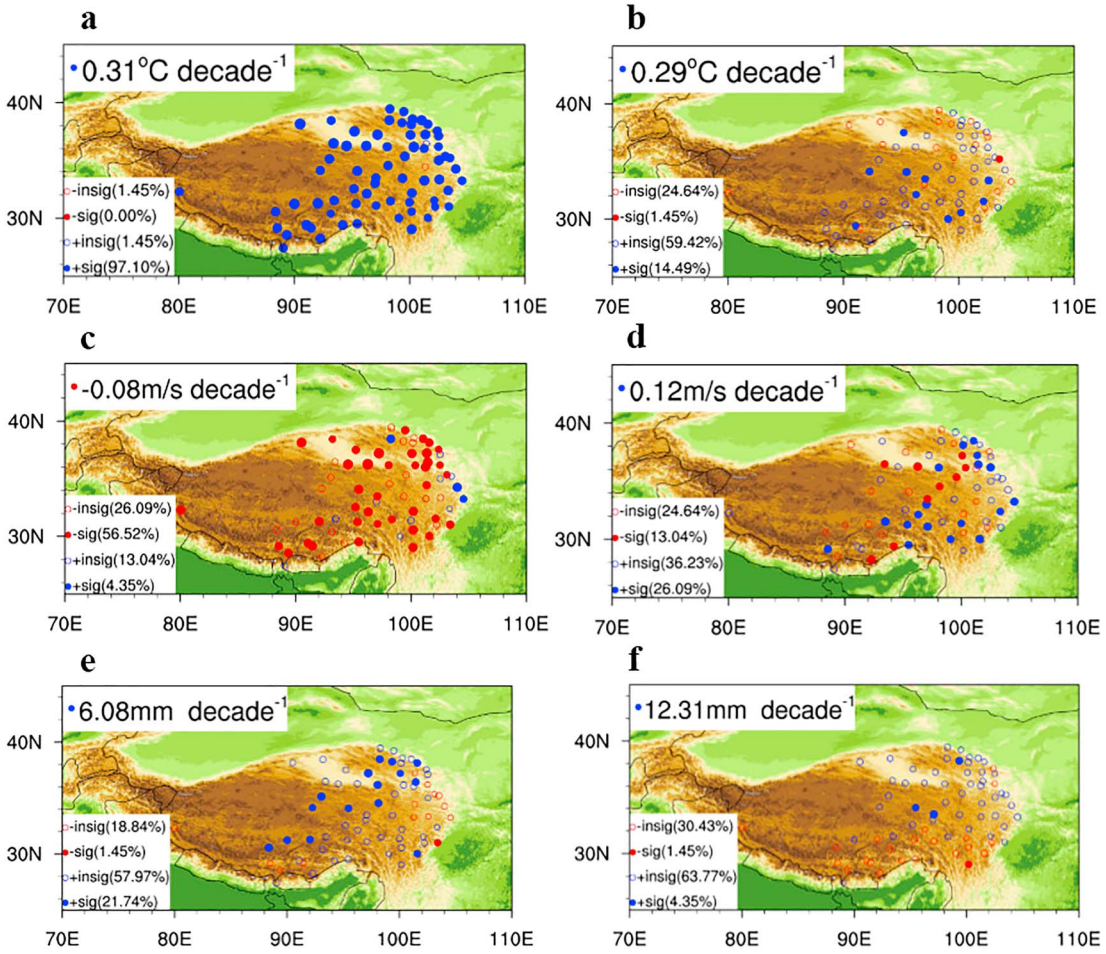

Figure 3. Spatial distribution of meteorological parameter trends at different time scales (a, b: air temperature; c, d: wind speed; e, f: precipitation; a, c, and e: long-term period from 1960–2014; b, d, and f: short-term time period from 1999–2014) over the Tibetan Plateau. Blue (red) circles denote positive (negative) trends. Closed circles indicate the 90% confidence level. The percentages of stations in the same trend category are given in parentheses. The average trends for each variable at different temporal scales are shown in the top left corner in each subfigure.

speed over the TP may cause a reduction in outward energy propagation, further raising the internal temperature over the TP (Yang et al., 2014). The third factor may be variations in cloud cover. Studies have shown that the total cloud cover over the TP is decreasing, while the nighttime low cloud cover is increasing (Duan & Wu, 2006; Wu et al., 2015). The daytime low cloud fraction and geometrical depth has decreased by approximately 4.2% and 130 m in recent years, respectively, based on observations by CloudSat and Cloud-Aerosol Lidar and Infrared Pathfinder Satellite Observations (Pan et al., 2017). A recent study (Liu et al., 2018) found that water vapor was the main driving force underlying the variations of mean temperature and minimum temperature by influencing downward longwave radiation. The sunshine duration was the driving source underlying the trend of maximum temperature and diurnal temperature range by altering the downward shortwave radiation. These changes will promote increases in plateau temperatures. The average wind speed decreased significantly in the long-term and midterm time periods (Figure 2c and Table 2). It should be noted that the wind speed increased significantly during the short-term time period (1999–2014), which was in marked contrast to the global wind stilling phenomena (Liepert, 2002; Stanhill & Moreshet, 1992; Vautard et al., 2010). The precipitation showed a general increasing trend, which is one of the signals of the wetting trend over the TP (Figure 2e and Table 2).

The M-K mutation and trend analysis results are shown in Figure 2. The average air temperature tended to decrease before 1968 (Figure 2b). Subsequently, it maintained an upward trend with some fluctuations. The air temperature increased significantly after 1994, when it reached the critical line representing a significance level of 0.01 (U = 2.58, thick dotted line). In the case of wind speed (Figure 2d), three phases

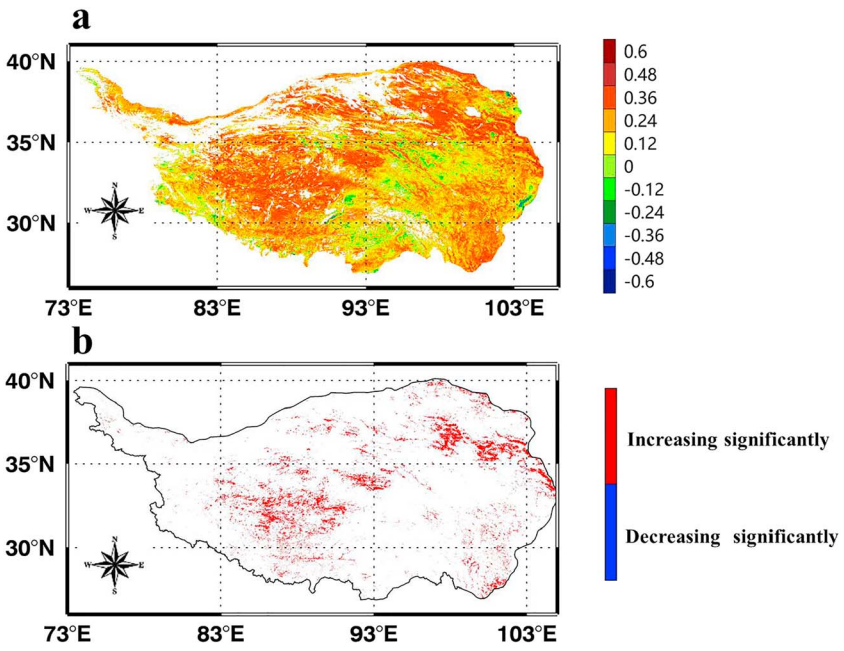

Figure 4. Spatial distribution of the linear trends of Normalized Difference Vegetation Index over the Tibetan Plateau (a) and their significance test results (b). The white color in (a) represents nonvegetation regions.

could be clearly identified. The wind speed decreased before 1963 and began to rise from 1964 to 1976, and then it subsequently decreased again. Over the entire study period, a sudden change occurred in 1993, and the wind stilling exceeded the critical line of 0.01 ($U = -2.58$) in 2000. The interannual variation of precipitation is obvious (Figure 2f), but the trend is not statistically significant in the midterm and short-term time periods.

General trends for the whole TP have been described above. Figure 3 helps to identify some details of the climate changing trends for every station involved in this study. In fact, differences were observed among the stations. For the long-term time scale, approximately 97.1% of stations showed significant increasing trends in air temperature (Figure 3a), while 56.52% stations showed significant weakening trends in wind speed (Figure 3c). However, a significant increase in precipitation was observed at only 21.74% of the stations, while insignificant increasing trends were observed in most stations (57.97%; Figure 3e). For the short-term time scale, air temperature increased at 73.91% stations, in which only 14.49% of stations passed the significance test (90% confidence level; Figure 3b). Wind speed recovered at 62.32% stations, in which 26.09% of stations passed the significance test (Figure 3d). As shown in Figures 3e and 3f, only a small proportion of stations passed the significance test and showed an increasing trend, whereas most stations showed insignificant variations, especially for the southeastern TP. This result is consistent with the conclusions of Feng and Zhou (2012), who indicated that the trend in summer precipitation over the southeastern TP from 1979–2002 was not significant

Table 3
Percentage of Significant Increases (90% Confidence Level) for Different Land Cover Types

Land Cover Type	Percentage (%)
Water	0.075
Evergreen needleleaf forest	0.0385
Evergreen broadleaf forest	0.0141
Deciduous needleleaf forest	0.0004
Deciduous broadleaf forest	0.0034
Mixed forest	0.3741
Closed shrublands	0.0069
Open shrublands	0.247
Woody savannas	0.0569
Savannas	0.0025
Grasslands	3.4968
Croplands	0.4993
Built-up	0.022
Barren	2.7798
Unclassified	0
Missing	0.0092

The TP has a complex topography and a wide range of glaciers and permafrost. The air temperature change with altitude is particularly noteworthy. The air temperature showed an overall increasing trend at different altitudes, with the rate of increase above 4,000 m being greater than that below 4,000 m during the midterm and short-term time periods (Table 2), which can be explained by the positive warming and albedo feedback caused by the melting of glaciers and snow cover at much higher elevations. The linear fitting of the curves for the three time periods (1960–2014, 1980–2014, and 1999–2014) showed that the rate of increase was greatest between 1980 and 2014.

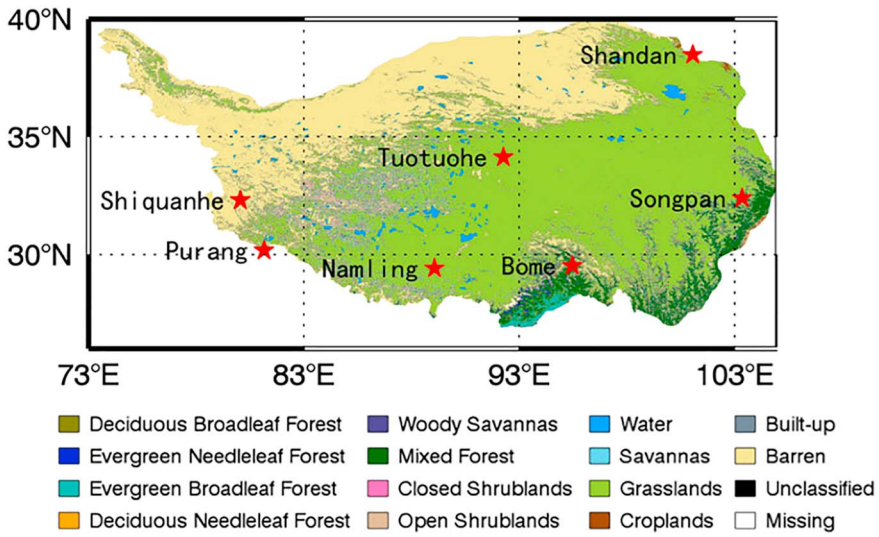

Figure 5. Land cover type of the TP and locations of seven selected stations.

3.2. Vegetation Response to Climate Change Over the TP

The TP is regarded as a region sensitive to climate change. A series of climatic changes have occurred at different time scales over the TP, which has inevitably led to changes in vegetation dynamics over this area. However, there is a lack of long-term cloud-free data for vegetation dynamics in the plateau. The optical remote sensing vegetation index has been widely used in plateau vegetation studies. However, the optical remote sensing vegetation index is influenced markedly by complex weather conditions over the plateau. Even the traditional MVC method cannot minimize cloud effects. Therefore, based on the HANTS algorithm and SPOT VGT data, a new cloud-free vegetation time series dataset from 1999–2014 has been reconstructed. The new vegetation dataset and the land cover data, both of which have the spatial resolution of 1 km, are used for analyzing the vegetation dynamics of all land cover types over the TP. The vegetation responses to short-term climate change over the TP were analyzed using this new dataset. According to the linear trend analysis, the vegetation density showed a general increasing trend under the background of TP warming (Figure 4a), which was observed over approximately 80% of the total Tibetan territory. It should be noted that some reforestation projects over the southern and eastern TP have been underway in recent decades, including the Natural Forest Conservation Program, which was implemented in 1998 (Zhang et al., 2000); the China Returning Farmland to Forest Project, which was launched in 1980s (Yin et al., 2004); and experimental reforestation trials on the southern slopes above Lhasa, which was launched in 1999 (Miehe et al., 2008). Such programs likely contributed to the increase in vegetation in the southeastern part of the TP; however, discerning natural and anthropogenic effects on vegetation dynamics is difficult. As shown in Table 3, a major significant increase was observed for the grasslands and barren land cover type in the western and northeastern part of the TP (Figure 4). Therefore, the major significant greening trend of the TP was mainly caused by climate factors. The reforestation projects mentioned above may have played a minor role in the vegetation greening in specific regions of the southwestern part of the TP.

Combined with the land cover information (Figure 5), three major increases were observed in the grassland, desert grassland, and mixed forest regions (40%, 22%, and 10%, respectively). Approximately 7.63% of the Tibetan territory showed significant increasing trends, while only 0.03% showed significant decreasing trends (90% confidence level). Most vegetation areas (89.07%) showed insignificant increasing trends, while others (3.27%) showed nonsignificant decreasing trends (Figures 4a and 4b). To investigate the dominant season for the wetting trend, we further calculated the trend for four seasons, and the results are shown as follows. For the northern and eastern part of the TP, the greening trend was dominant in summer (Figures 6c and 6g). For the southwestern TP, the greening trend is dominant in winter, spring, and summer (Figures 6a, 6b, 6d–6f, and 6h). The general wetting and greening trend of the TP revealed by our study is consistent with several former studies (e.g., Ding et al., 2007; Zhang et al., 2017). Due to the differences in

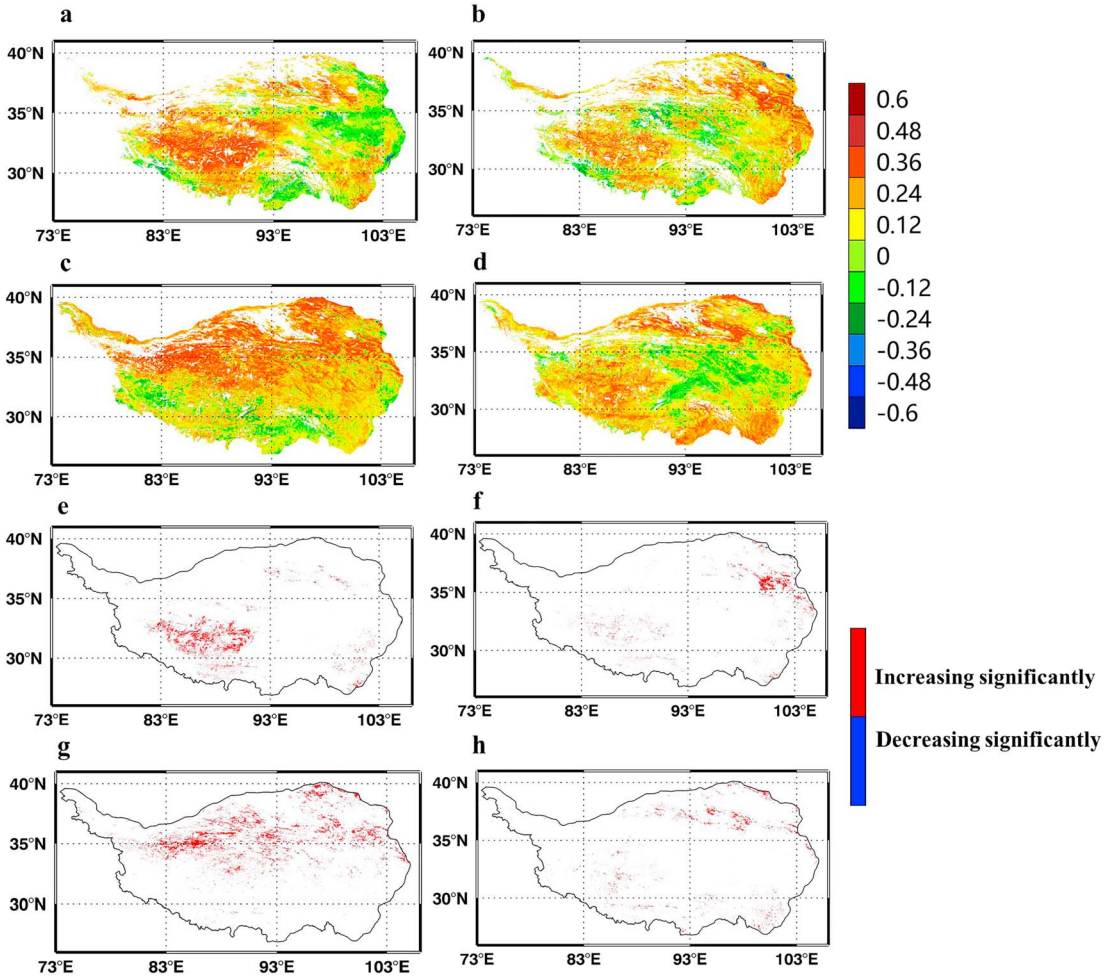

Figure 6. Spatial distribution of the linear trends of Normalized Difference Vegetation Index and their significant test results from 1999 to 2014 over the Tibetan Plateau for winter (a and e, December, January, and February), spring (b and f, March, April, and May), summer (c and g, June, July, and August), and autumn (d and h, September, October, and November).

the study periods and NDVI data sources, some discrepancies are observed among these studies. For example, Ding et al. (2007) identified an increase in the NDVI in the southern and eastern TP. Zhang et al. (2017) found that the wetting and greening of the TP occurred in early summer. Our study revealed that the wetting and greening trends have heterogeneous characteristics. The greening trends varied with the season and spatial location. As shown in Figure 4, a significant increase in the NDVI occurred in the northeastern and southwestern part of the TP.

Table 4
Seven Meteorological Sites and Their Relevant Information

Station	LCT	Elevation (m)	NDVI	Air temperature (°C)	Precipitation (mm)	Relative humidity (%)	Sunshine duration (hr)	Climatic region
Shiquanhe	Sparsely vegetated	4,278.6	0.093	1.703	70.787	31.495	3,493.873	Arid
Purang	Grassland	4,900	0.099	4.249	154.007	45.205	3,158.827	Arid
Shandan	Grassland	1,764.6	0.154	7.519	207.720	46.045	2,852.400	Semiarid
Tuotuohe	Grassland	4,533.1	0.179	−3.007	338.067	52.583	2,894.573	Semiarid
Namling	Open shrublands	4,000	0.117	6.297	510.353	42.545	2,912.827	Semihumid
Songpan	Evergreen needleleaf	2,850.7	0.499	6.673	707.427	62.061	1,747.427	Semihumid
Bome	Mixed forests	2,736	0.698	9.354	841.480	69.828	1,461.173	Humid

Note. NDVI = Normalized Difference Vegetation Index; LCT = land cover type.

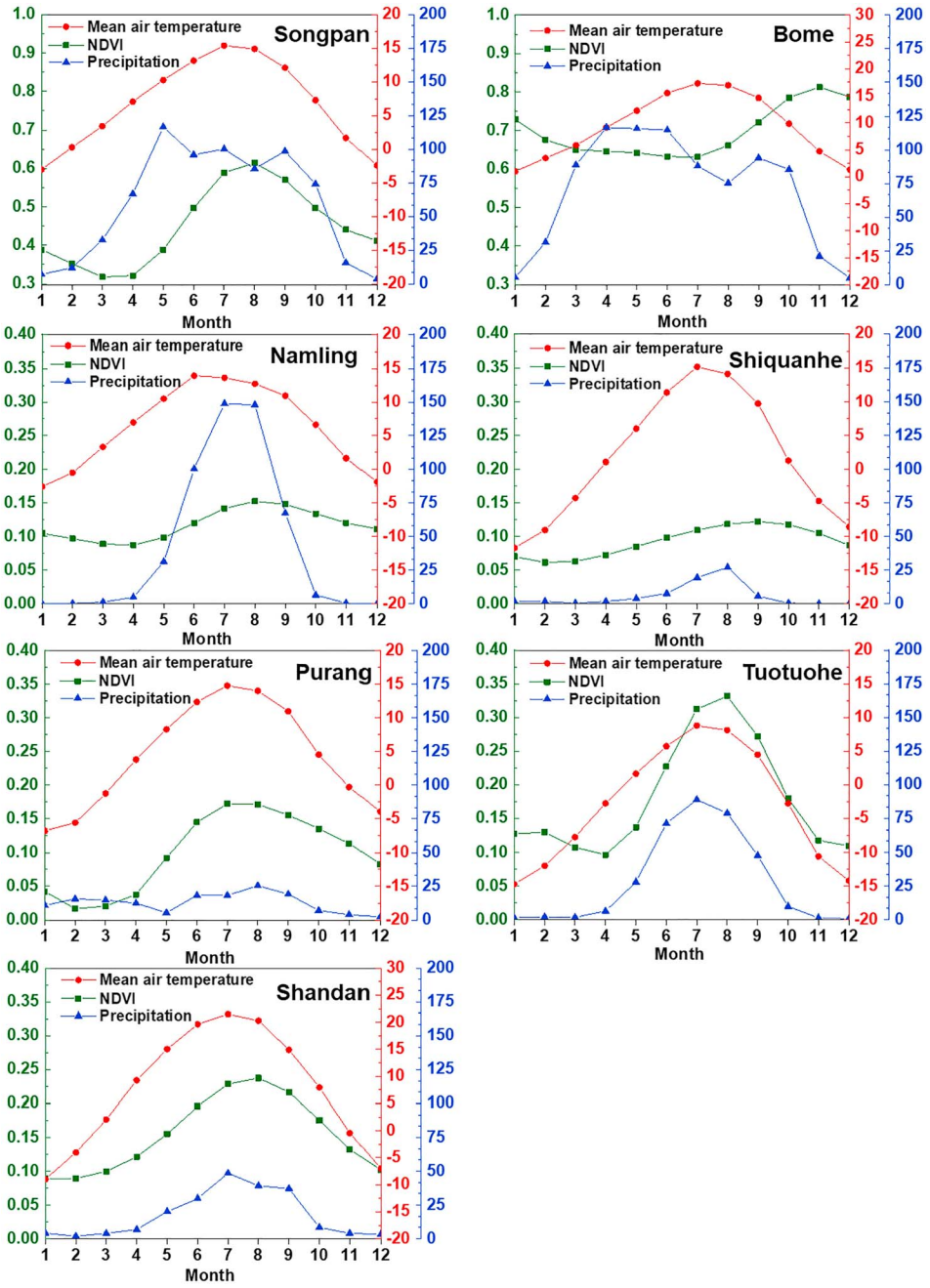

Figure 7. Time series of NDVI (green), air temperature (°C, red), and precipitation (mm, blue) for seven stations. NDVI = Normalized Difference Vegetation Index.

To understand the physical mechanisms underlying the vegetation changes, we analyzed the relationship of vegetation changes with temperature and precipitation over different land types. Since the temporal coverage of SPOT VGT started in 1999, observations from 1999–2014 for more than 69 stations could be introduced here. Combined with vegetation coverage data (MOD12Q1) and meteorological data (air temperature and precipitation) in the short-term time period, seven meteorological stations over five major land cover types were selected to study the relationship between vegetation density and meteorological parameters (Table 4 and Figure 5). The seven selected stations belong to four climatic zones: arid, semiarid, semihumid, and humid. Figure 7 shows the time series of the vegetation index, temperature index, and

Table 5
Correlation Coefficients Between NDVI and Meteorological Parameters During 1999–2014

Station	Mean air temperature	Precipitation
Shiquanhe	0.687	0.511
Purang	0.832	0.338
Shandan	0.901	0.928
Tuotuohe	0.831	0.925
Namling	0.546	0.721
Songpan	0.707	0.555
Bome	0.675	0.117

Note. NDVI = Normalized Difference Vegetation Index.

precipitation index for each station. The air temperature at seven stations showed a one-peak distribution, with a maximum in summer. The precipitation at Songpan and Bome showed a bimodal distribution, while the precipitation at the other five stations showed a unimodal distribution. The variations in air temperature, precipitation, and NDVI are more consistent after the freeze-thaw period. For most stations, the increase in the NDVI usually lags one to two months behind the changes in air temperature and precipitation. The Bome station is located in a humid region at a lower altitude; therefore, the variation in vegetation mainly depends on energy-related factors. The correlation between the vegetation index and in situ meteorological data (Table 5) showed that a significant correlation occurred between air temperature and the majority of underlying surface vegetation growth. The relationship between precipitation and vegetation was diverse. In addition, the different response characteristics of various vegetation types were significant. For example, semiarid grassland vegetation (such as that of the Shandan and Tuotuohe stations) was extremely sensitive to air temperature and precipitation in general. In particular, the correlation coefficients of the Shandan Station were the highest among all vegetation types, indicating that the main limiting factors for vegetation growth in this area were air temperature and precipitation. With regard to the desert grassland in the arid region (Shiquanhe), grassland (Purang), semihumid evergreen coniferous forest (Songpan), and humid mixed forest (Bome), vegetation growth was mainly influenced by temperature. The impacts of precipitation did not pass the significance test. The open bush (Namling) in the semihumid region was mainly influenced by precipitation. With a combination of better water and heat conditions (Bome Station), vegetation growth was still significantly correlated with air temperature, although the correlation was less significant than in the semiarid grassland regions, such as Shandan and Tuotuohe, indicating that precipitation and temperature were not the limiting factors of local vegetation growth. As can also be seen from Figure 8, the air temperature dominated the summer greening change at Tuotuohe station. It should be noted that the Arctic ecosystems, which are similar to the ecosystems in the TP, were also found to have a trend of greening with the increasing in Arctic air temperatures (Chapin et al., 2005; Pearson et al., 2013). Continued greening will produce multiple climate feedbacks. For instance, increased vegetation coverage reduces albedo, which cause increased surface net short-wave radiation. Second, higher evapotranspiration will increase atmospheric water vapor concentrations, which will lead to more downward longwave radiation. This is another positive feedback. Simultaneously, more evapotranspiration will cause a cooling effect. In Arctic region, the positive feedback of vegetation greening play a major role with Arctic warming. However, the cooling effect, especially for daytime cooling, has been verified to be dominant in the TP for the growing season by using a regional climate model (Shen et al., 2015). It should be noted that the relationship between vegetation activity and temperature variability can be modulated or changed with many other factors involved, such as precipitation, insects, snow cover, overgrazing, and changes in nutrient availability (Piao et al., 2014). In other words, a nonlinear relationship exists between vegetation and temperature. The influence of future climate change on the vegetation dynamics over the TP needs to be further investigated. We speculate some vegetation cover will shift to different classes. However, further investigations need to be carried out by using different climate models or Earth system models.

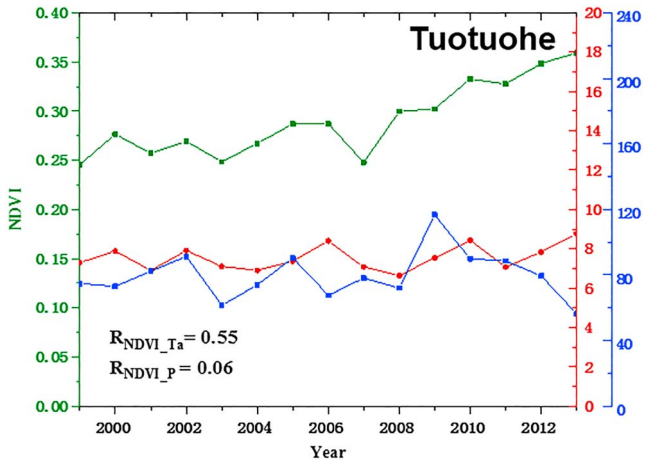

Figure 8. Time series of summer mean NDVI (green), air temperature (°C, red), and precipitation (mm, blue) at Tuotuohe station. NDVI = Normalized Difference Vegetation Index.

4. Concluding Remarks

A consistent warming trend was identified for different time periods (long term: 1960–2014; midterm: 1980–2014; short term 1999–2014) through analyses of a variety of observation indexes of the climate system over the TP. The air temperature over the TP was 1.27 °C higher than normal since 2014. The average increase was 2.2 times the global average (0.57 °C). The results of this study showed that a warming slowdown

phenomenon had occurred over the TP. The warming rate in high-altitude regions of the TP (>4,000 m) was 1–2 times higher than that in the low-altitude regions (<4,000 m). The results of the M-K analysis indicated marked interdecadal variation in air temperature in the TP. The physical mechanism of TP warming can be explained by a decrease in the plateau surface albedo, weakening of the wind speed, decrease in the low cloud fraction and geometrical depth and increase in the nighttime low cloud coverage. The significant increase in TP temperature, especially in high-altitude areas, will cause accelerated changes in plateau glaciers and snow cover, which will have a profound influence on the hydrological cycle of the TP. Compared with plateau warming, precipitation showed an insignificant increasing rate in the midterm and short-term time periods, and an interdecadal oscillation occurred during all time periods in the TP. The wind speed of the TP had a significant weakening trend in the long-term and midterm periods, and there was a sudden change in 1995. However, there were signals of recent recovery in wind speed. With short-term warming and increasing precipitation over the TP, a general increasing trend of vegetation density from 1999 to 2014 was identified from satellite data. The region showing increases accounted for approximately 80% of the total Tibetan territory, while the region showing significant increases accounted for 7.63%.

Because of the large number of underlying vegetation types over the TP, differential responses were obvious. Generally, the vegetation types in high-altitude cold areas were temperature sensitive, whereas their relationship with precipitation was nonsignificant. The grassland in semiarid regions was the dominant vegetation type over the TP, and its correlation coefficients with temperature and precipitation significantly exceeded those of the other vegetation types in the semihumid region, which had considerably superior hydrothermal conditions.

Acknowledgments
We thank the three anonymous reviewers for their comments, which have helped us greatly improve the manuscript. This research was jointly funded by Strategic Priority Research Program of Chinese Academy of Sciences (Grant XDA20060101), the National Natural Science Foundation of China (Grants 41875031, 41522501, 41275028, 41661144043, and 91837208), the Chinese Academy of Sciences (Grant QYZDJ-SSW-DQC019), and CLIMATE-TPE (ID 32070) in the framework of the ESA-MOST Dragon 4 Programme. The author would also like to thank China Meteorological Administration for their data sharing program. The in situ meteorological data was obtained from the Chinese Meteorological Data Network (http://data.cma.gov.cn/). The SPOT vegetation data can be downloaded from the VITO Product Distribution Portal (https://www.vito-eodata.be).

References

An, Z. S., Colman, S. M., Zhou, W., Li, X., Brown, E. T., Jull, A. J. T., et al. (2012). Interplay between the Westerlies and Asian monsoon recorded in Lake Qinghai sediments since 32 ka. *Scientific Reports*, *2*(1). https://doi.org/10.1038/srep00619

Chapin, F. S. 3rd, Sturm, M., Serreze, M. C., McFadden, J. P., Key, J. R., Lloyd, A. H., et al. (2005). Role of land-surface changes in arctic summer warming. *Science*, *310*(5748), 657–660. https://doi.org/10.1126/science.1117368

Climate Change Center of China Meteorological Administration (2015). *China climate change monitoring bulletin*. Beijing: China Meteorological Administration.

Ding, M., Zhang, Y., Liu, L., Zhang, W., Wang, Z., & Bai, W. (2007). The relationship between NDVI and precipitation on the Tibetan Plateau. *Journal of Geographical Sciences*, *17*(3), 259–268. https://doi.org/10.1007/s11442-007-0259-7

Duan, A. M., & Wu, G. X. (2006). Changes of cloud amount and the climate warming on the Tibetan Plateau. *Geophysical Research Letters*, *33*, L22704. https://doi.org/10.1029/2006GL027946

Easterling, D. R., & Wehner, M. F. (2009). Is the climate warming or cooling? *Geophysical Research Letter*, *36*, L08706. https://doi.org/10.1029/2009GL037810

Feng, L., & Zhou, T. (2012). Water vapor transport for summer precipitation over the Tibetan Plateau: Multidata set analysis. *Journal of Geophysical Research*, *117*, D20114. https://doi.org/10.1029/2011JD017012

Friedl, M. A., Sulla-Menashe, D., Tan, B., Schneider, A., Ramankutty, N., Sibley, A., & Huang, X. (2010). MODIS Collection 5 global land cover: Algorithm refinements and characterization of new datasets. *Remote Sensing of Environment*, *114*(1), 168–182. https://doi.org/10.1016/j.rse.2009.08.016

Gerstengarbe, F. W., & Werner, P. C. (1999). Estimation of the beginning and end of recurrent events within a climate regime. *Climate Research*, *11*, 97–107. https://doi.org/10.3354/cr011097

Huang, K., Zhang, Y., Zhu, J., Liu, Y., Zu, J., & Zhang, J. (2016). The influences of climate change and human activities on vegetation dynamics in the Qinghai-Tibet Plateau. *Remote Sensing*, *8*(10). https://doi.org/10.3390/rs8100876

Immerzeel, W., Quiroz, R., & Jong, S. (2005). Understanding precipitation patterns and land use interaction in Tibet using harmonic analysis of SPOT VGT-S10 NDVI time series. *International Journal of Remote Sensing*, *26*(11), 2281–2296. https://doi.org/10.1080/01431160512331326611

Intergovernmental Panel on Climate Change (2013). *Climate change 2013: The physical science basis*. Cambridge: Cambridge University Press.

Kang, S. C., Xu, Y. W., You, Q. L., Flugel, W. A., Pepin, N., & Yao, T. D. (2010). Review of climate and cryospheric change in the Tibetan Plateau. *Environmental Research Letters*, *5*(1). https://doi.org/10.1088/1748-9326/5/1/015101

Kendall, M. G. (1975). *Rank correlation methods*. London: Griffin.

Kerr, R. A. (2009). What happened to global warming? Scientists say just wait a bit. *Science*, *326*(5949), 28–29. https://doi.org/10.1126/science.326_28a

Knight, J., Kennedy, J. J., Folland, C., Harris, G., Jones, G. S., Palmer, M., et al. (2009). Do global temperature trends over the last decade falsify climate predictions? *Bulletin of the American Meteorological Society*, *90*(8), S22–S23.

Kosaka, Y., & Xie, S. P. (2013). Recent global-warming hiatus tied to equatorial Pacific surface cooling. *Nature*, *501*(7467), 403–407. https://doi.org/10.1038/nature12534

Li, Q., Zhang, L., Xu, W., Zhou, T., Wang, J., Zhai, P., & Jones, P. (2017). Comparisons of time series of annual mean surface air temperature for china since the 1900s: Observations, model simulations, and extended reanalysis. *Bulletin of the American Meteorological Society*, *98*(4), 699–711. https://doi.org/10.1175/BAMS-D-16-0092.1

Liepert, B. G. (2002). Observed Reductions in Surface Solar Radiation in the United States and Worldwide from 1961 to 1990. *Geophysical Research Letters*, *29*(10), 1421. https://doi.org/10.1029/2002GL014910

Liu, Y., Zhang, Y., Zhu, J., Huang, K., Zu, J., Chen, N., et al. (2018). Warming slowdown over the Tibetan plateau in recent decades. *Theoretical and Applied Climatology*, *135*(3-4), 1375–1385. https://doi.org/10.1007/s00704-018-2435-3

Liu, Z. Y., Li, C., Zhou, P., & Chen, X. Z. (2016). A probabilistic assessment of the likelihood of vegetation drought under varying climate conditions across China. *Scientific Reports*, *6*(1). https://doi.org/10.1038/srep35105

Maisongrande, P., Duchemin, B., & Dedieu, G. (2004). VEGETATION/SPOT: An operational mission for the Earth monitoring; presentation of new standard products. *International Journal of Remote Sensing*, *25*(1), 9–14. https://doi.org/10.1080/0143116031000115265

Mann, H. B. (1945). Nonparametric tests aginst trend. *Econometrica*, *13*(3), 245–259. https://doi.org/10.2307/1907187

Meehl, G. A., Arblaster, J. M., Fasullo, J. T., Hu, A. X., & Trenberth, K. E. (2011). Model-derived evidence of deep-ocean heat uptake during surface-temperature hiatus periods. *Nature Climate Change*, *1*(7), 360–364. https://doi.org/10.1038/nclimate1229

Miehe, G., Miehe, S., Will, M., Opgenoorth, L., Duo, L., Dorgeh, T., & Liu, J. (2008). An inventory of forest relicts in the pastures of Southern Tibet (Xizang AR, China). *Plant Ecology*, *194*(2), 157–177.

Pan, Z., Mao, F., Gong, W., Min, Q., & Wang, W. (2017). The warming of Tibetan Plateau enhanced by 3D variation of low-level clouds during daytime. *Remote Sensing of Environment*, *198*, 363–368. https://doi.org/10.1016/j.rse.2017.06.024

Pearson, R. G., Phillips, S. J., Loranty, M. M., Beck, P. S. A., Damoulas, T., Knight, S. J., & Goetz, S. J. (2013). Shifts in Arctic vegetation and associated feedbacks under climate change. *Nature Climate Change*, *3*(7), 673–677. https://doi.org/10.1038/nclimate1858

Piao, S., Nan, H., Huntingford, C., Ciais, P., Friedlingstein, P., Sitch, S., et al. (2014). Evidence for a weakening relationship between interannual temperature variability and northern vegetation activity. *Nature Communications*, *5*(1). https://doi.org/10.1038/ncomms6018

Rees, M., Condit, R., Crawley, M., Pacala, S., & Tilman, D. (2001). Long-term studies of vegetation dynamics. *Science*, *293*(5530), 650–655. https://doi.org/10.1126/science.1062586

Shen, M., Piao, S., Jeong, S. J., Zhou, L., Zeng, Z., Ciais, P., et al. (2015). Evaporative cooling over the Tibetan Plateau induced by vegetation growth. *Proceedings of the National Academy of Sciences of the United States of America*, *112*(30), 9299–9304. https://doi.org/10.1073/pnas.1504418112

Stanhill, G., & Moreshet, S. (1992). Global radiation climate changes in Israel. *Climatic Change*, *22*(2), 121–138. https://doi.org/10.1007/BF00142962

Sun, Y. L., Yang, Y. L., Zhang, L., & Wang, Z. L. (2015). The relative roles of climate variations and human activities in vegetation change in North China. *Physics and Chemistry of the Earth*, *87-88*, 67–78. https://doi.org/10.1016/j.pce.2015.09.017

Tian, F., Brandt, M., Liu, Y. Y., Rasmussen, K., & Fensholt, R. (2017). Mapping gains and losses in woody vegetation across global tropical drylands. *Global Change Biology*, *23*(4), 1748–1760. https://doi.org/10.1111/gcb.13464

Trenberth, K. E., & Fasullo, J. T. (2013). An apparent hiatus in global warming? *Earth's Future*, *1*(1), 19–32. https://doi.org/10.1002/2013EF000165

Vautard, R., Cattiaux, J., Yiou, P., Thepaut, J. N., & Ciais, P. (2010). Northern Hemisphere atmospheric stilling partly attributed to an increase in surface roughness. *Nature Geoscience*, *3*(11), 756–761. https://doi.org/10.1038/ngeo979

Verhoef, W. (1996). Application of harmonic analysis of NDVI Time Series (HANTS). In S. Azzali, & M. Menenti (Eds.), *Fourier analysis of temporal NDVI in the Southern African and American continents* (pp. 19–24, Report 108). Wageningen, The Netherlands: DLO Winand Staring Centre.

Wang, H., Liu, D., Lin, H., Montenegro, A., & Zhu, X. (2015). NDVI and vegetation phenology dynamics under the influence of sunshine duration on the Tibetan plateau. *International Journal of Climatology*, *35*(5), 687–698. https://doi.org/10.1002/joc.4013

Wen, J., Su, Z., & Ma, Y. (2004). Reconstruction of a cloud-free vegetation index time series for the Tibetan Plateau. *Mountain Research and Development*, *24*(4), 348–353.

Wu, H., Yang, K., Niu, X. L., & Chen, Y. Y. (2015). The role of cloud height and warming in the decadal weakening of atmospheric heat source over the Tibetan Plateau. *Science in China Series D: Earth Sciences*, *58*(3), 395–403. https://doi.org/10.1007/s11430-014-4973-6

Xie, S. P. (2016). OCEANOGRAPHY Leading the hiatus research surge. *Nature Climate Change*, *6*(4), 345–346. https://doi.org/10.1038/nclimate2973

Xu, Z., Gong, T., & Li, J. (2008). Decadal trend of climate in the Tibetan Plateau-regional temperature and precipitation. *Hydrological Processes*, *22*(16), 3056–3065. https://doi.org/10.1002/hyp.6892

Yang, K., Wu, H., Qin, J., Lin, C. G., Tang, W. J., & Chen, Y. Y. (2014). Recent climate changes over the Tibetan Plateau and their impacts on energy and water cycle: A review. *Global and Planetary Change*, *112*, 79–91. https://doi.org/10.1016/j.gloplacha.2013.12.001

Yao, T. D., Liu, X. D., Wang, N. L., & Shi, Y. F. (2000). Amplitude of climatic changes in Qinghai-Tibetan Plateau. *Chinese Science Bulletin*, *45*(13), 1236–1243. https://doi.org/10.1007/BF02886087

Yin, J., Liu, C., Zhao, W., & He, K. (2004). Tree productivity and water potential productivity in returning farmland to forest project in Datong County, Qinghai Province. *Forestry Studies in China*, *6*(3), 36–42. https://doi.org/10.1007/s11632-004-0038-9

Zhang, P., Shao, G., Zhao, G., Le Master, D. C., Parker, G. R., Dunning, J. B., & Li, Q. (2000). China's forest policy for the 21st century. *Science*, *288*(5474), 2135–2136. https://doi.org/10.1126/science.288.5474.2135

Zhang, W., Zhou, T., & Zhang, L. (2017). Wetting and greening Tibetan Plateau in early summer in recent decades. *Journal of Geophysical Research: Atmospheres*, *122*, 5808–5822. https://doi.org/10.1002/2017JD026468

Zhong, L., Su, Z., Ma, Y., Salama, M. S., & Sobrino, J. A. (2011). Accelerated changes of environmental conditions on the Tibetan Plateau caused by climate change. *Journal of Climate*, *24*(24), 6540–6550. https://doi.org/10.1175/JCLI-D-10-05000.1

Zhu, J., Zhang, Y., & Jiang, L. (2016). Experimental warming drives a seasonal shift of ecosystem carbon exchange in Tibetan alpine meadow. *Agricultural and Forest Meteorology*, *233*, 242–249.

Zhu, Z., Piao, S., Myneni, R. B., Huang, M., Zeng, Z., Canadell, J. G., et al. (2016). Greening of the Earth and its drivers. *Nature Climatic Change*, *6*(8), 791–795. https://doi.org/10.1038/NCLIMATE3004

Zou, M., Zhong, L., Ma, Y., Hu, Y., Huang, Z., Xu, K., & Feng, L. (2018). Comparison of two satellite-based evapotranspiration models of the Nagqu River Basin of the Tibetan Plateau. *Journal of Geophysical Research: Atmospheres*, *123*, 3961–3975. https://doi.org/10.1002/2017JD027965